

## LUMINOSITY INDICATORS IN THE SPECTRA OF QUASI-STELLAR OBJECTS\*

JACK A. BALDWIN

Lick Observatory, Board of Studies in Astronomy and Astrophysics, University of California, Santa Cruz  
 Received 1976 September 24

### ABSTRACT

Spectrophotometric observations were made of 20 quasi-stellar objects having redshifts in the range  $z = 1.24$ – $3.53$ . Continuum luminosities were calculated on the assumption that the redshifts are cosmological, and several features of the emission lines were tested as possible luminosity indicators. A strong correlation is found between the continuum luminosities and the equivalent widths of the emission lines, but it is not clear to what extent this may be a selection effect.

*Subject heading:* quasars

### I. INTRODUCTION

For the 15 years since their discovery, quasi-stellar radio sources have been eyed by observational cosmologists as potentially very useful standard candles because of their visibility out to large redshifts. Unfortunately, the very large scatter of these objects on the redshift-magnitude diagram indicates that if the redshifts are indeed cosmological in origin, there must be a wide range in luminosity which masks the cosmological effects. Bahcall and Hills (1973) studied the upper envelope of the QSO redshift-magnitude diagram and concluded that the observations are at least consistent with the cosmological redshift hypothesis; but as has been pointed out by Burbidge (1973), this certainly does not prove the case. Setti and Woltjer (1973a) found that for QSOs with steep radio spectra, the redshift-magnitude diagram has the appearance of a noisy linear relationship with about the correct slope for  $q_0 = +1$  but with a scatter of at least 2 mag. Stannard (1973) found a similar result for QSOs with flat radio spectra, but the implied mean luminosity was about 1 mag brighter than for the QSOs with steep radio spectra. Radio-quiet QSOs and QSOs with concave radio spectra were found not to show any correlation between redshift and apparent magnitude which could be attributed to cosmological effects.

This paper reports the results of a search for a more precise luminosity indicator which might be used to refine the Hubble diagram for QSOs. Careful measurements were made of several emission features and of the continuum flux in the optical spectra of a number of QSOs. The results show that there is in fact a strong correlation between the continuum luminosity and the equivalent width of the emission lines, but it is not clear to what extent this may be a selection effect.

### II. OBSERVATIONS

The QSOs in this sample were selected primarily from published lists so that objects scattered all over

\* *Lick Observatory Bulletin*, No. 748.

the redshift-magnitude diagram would be included in the observations (Fig. 1). An initial sample was chosen with a range of redshifts such that the  $L\alpha$  emission line could always be observed, but a few additional QSOs at slightly lower redshifts were added to the sample at a later date. The observations were made at the Cassegrain focus of the Lick Observatory 120 inch (3 m) telescope with the image-tube scanner system (Robinson and Wampler 1971); resolutions of about 7 and 15 Å were used. Table 1 lists the observed objects and some details of the observations, while Table 2 lists some results (reduced to the rest frames of the QSOs). Observational material taken from other sources is also given in Table 1.

The observations were made through  $2'' \times 2''$  entrance apertures which gave a resolution of about 7 Å full width at half-maximum (FWHM); observations were then usually repeated through  $4'' \times 4''$  or

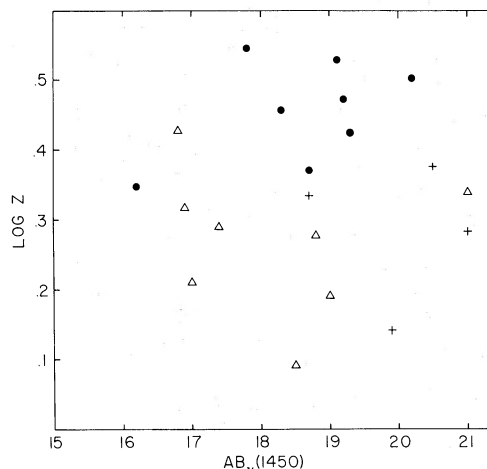


FIG. 1.—Redshift-magnitude diagram for the QSOs included in this study.  $AB_v(1450)$  is the continuum magnitude observed at a wavelength corresponding to 1450 Å in the rest frame of each object. Filled circles represent flat radio spectra; crosses, steep radio spectra; triangles, concave or radio-quiet spectra.

TABLE 1  
JOURNAL OF OBSERVATIONS

| Object      | Reference | Radio Spectrum | Reference | Dates Observed  |
|-------------|-----------|----------------|-----------|---|
| BSO 1       | 1         | Quiet          | 9         | 27 Feb 76*, 26 Mar 76*  |
| 3C 181      | 1         | Steep          | 9         | 27 Feb 76*, 26 Mar 76   |
| 4C 31.38    | 1         | Concave        | 9         | 27 Feb 76*  |
| Ton 490     | 1         | Concave        | 10        | 27 Feb 76*, 26 Mar 76*  |
| 1548+115b   | 2         | Quiet          | 11        | 27 Feb 76*, plus data taken from Wampler et al (1973a)  |
| 4C 29.50    | 1         | Steep          | 9         | 8 Aug 75, 9 Aug 75, 10 Aug 75, 1 Sept 75  |
| PHL 938     | 1         | Quiet          | 9         | 6 Oct 72, 14 Sept 74*, 12 Nov 74*, 17 Dec 74*, 13 Jan 75*   |
| 1331+170    | 3         | Concave        | 12        | Data taken from Strittmatter et al (1973)   |
| PKS 0424-13 | 1         | Steep          | 9         | 11 Nov 74, 12 Jan 75*, 13 Jan 75*   |
| 1108+285    | 1         | Quiet          | 9         | 29 Jan 76   |
| B1225+31.7  | 4         | Flat           | 4         | Data taken from Wampler et al (1976)  |
| 4C 25.05    | 1         | Flat           | 9         | 12 Nov 74*, 17 Dec 74*, 8 Aug 75*, 9 Aug 75*, 10 Aug 75, 2 Oct 75, 28 Jan 76*   |
| 5C 2.56     | 1         | Steep          | 9         | 28 Jan 76, 29 Jan 76*   |
| 2256+017    | 3         | Flat           | 13        | 4 Sept 72, 4 Oct 73, 28 Oct 73, 10 Nov 74, 12 Nov 74, 7 Aug 75*, 8 Aug 75, 9 Aug 75, 10 Aug 75, 1 Sept 75, 2 Oct 75, 3 Oct 75 |
| PHL 957     | 1         | Quiet          | 9         | 7 Dec 75*, plus data taken from Coleman et al (1976)  |
| 4C 05.34    | 1         | Flat           | 9         | 2 Mar 73, 28 Oct 73, 4 Nov 74, 11 Nov 74*, 7 Dec 75*  |
| 0830+115    | 5         | Flat           | 5         | 17 Dec 74, 13 Jan 75*, 7 Dec 75*, 29 Jan 76*  |
| 0938+119    | 6         | Flat           | 5         | 13 Jan 75, 28 Jan 76*, 28 Feb 76  |
| 0H471       | 7         | Flat           | 14        | 2 Oct 75, 3 Oct 75, 6 Dec 75, 28 Jan 76   |
| 0Q172       | 8         | Flat           | 12,14     | Data taken from Baldwin et al (1974)  |

\* indicates at least part of data obtained through large entrance aperture.

|             |                           |                                      |   |
|-------------|---------------------------|--------------------------------------|---|
| References: | 1 = De Veny et al (1971)  | 6 = Beaver et al (1976)              | 11 = Argue et al (1974)                         |
|             | 2 = Wampler et al (1973a) | 7 = Carswell and Strittmatter (1973) | 12 = Murdoch (1974)                             |
|             | 3 = Baldwin et al (1973)  | 8 = Wampler et al (1973b)            | 13 = I. W. A. Browne<br>(private communication) |
|             | 4 = Fanti et al (1975)    | 9 = Setti and Woltjer (1973b)        | 14 = Gearhart et al (1974)                      |
|             | 5 = Baldwin et al (1976)  | 10 = Hoskins et al (1974)            |   |

6" × 6" apertures in order to make accurate flux measurements. The scans were calibrated by using the larger entrance apertures to scan standard stars from the list observed by Stone (1974). The continuum fluxes measured through the larger apertures were generally found to be repeatable to at least 10% or better, and the error bars given in Table 2 represent the rms deviations for photometric nights. It was not possible to make these careful measurements with the larger apertures for some of the faintest QSOs in the sample; but the light loss could be estimated from the scans of the brighter QSOs, and the size of the error bars in Table 2 have been increased correspondingly.

The equivalent widths listed in Table 2 are tabulated in the rest frames of the QSOs and were measured from weighted sums of all of the higher-resolution

scans of each object. The principal uncertainty lies in where the continuum level should be drawn. To make sure that the possible errors were not underestimated, equivalent widths of the C IV lines were measured from the scans for each individual night, and the error bars given in Table 2 are the weighted rms deviations of these individual determinations. The actual errors should be smaller because the final measurements were made from summed data having a higher signal-to-noise ratio than any of the individual scans.

### III. RESULTS

A preliminary analysis of the data was made in an attempt to find correlations between the continuum magnitudes and possibly relevant parameters of the

TABLE 2  
OBSERVATIONAL RESULTS

| Object      | Redshift | $AB_v(\lambda_0 1450)$ | $\log L_{\text{cont}}$<br>$\log(\text{erg s}^{-1} \text{H}_\alpha^{-1})$ | Rest Frame                             |  |  |                              |                  |
|-------------|----------|------------------------|--|--|--|--|------------------------------|------------------|
|             |          |                        |  | $\log W_\lambda$<br>(Ly- $\alpha$ +NV) | $\log W_\lambda$<br>(C IV $\lambda 1550$ ) | $\log W_\lambda$<br>(C III] $\lambda 1909$ ) | I(C IV)/<br>I(Ly- $\alpha$ ) | FWHM<br>(C IV)   |
|             |          |                        |  | [log( $\text{\AA}$ )]                  | [log( $\text{\AA}$ )]                      | [log( $\text{\AA}$ )]                        |                              | ( $\text{\AA}$ ) |
| BSO 1       | 1.24     | 18.5 $\pm$ .3          | 30.63 $\pm$ .13  |  | 1.54                                       |  |                              | 30               |
| 3C 181      | 1.38     | 19.9 $\pm$ .3          | 30.13 $\pm$ .12  |  | 2.07                                       |  |                              | 29               |
| 4C 31.38    | 1.56     | 19:                    | 30.57:   |  | 1.57                                       |  |                              | 23               |
| Ton 490     | 1.63     | 17.0 $\pm$ .3          | 31.39 $\pm$ .12  |  | 1.65                                       |  |                              | 24               |
| 1548+115b   | 1.90     | 18.8:                  | 30.77:   | 1.90:                                  | 1.57 $\pm$ .03                             | 1.46   | .42:                         | 27 $\pm$ 1       |
| 4C 29.50    | 1.92     | 21.0 $\pm$ .3          | 29.89 $\pm$ .12  | 2.25                                   | 2.18 $\pm$ .05                             | 1.57   | .56                          | 23 $\pm$ 1       |
| PHL 938     | 1.95     | 17.4 $\pm$ .1          | 31.34 $\pm$ .04  | 1.71                                   | 1.51 $\pm$ .07                             | 1.28   | .45                          | 33 $\pm$ 1       |
| 1331+170    | 2.08     | 16.9:                  | 31.58:   | 1.90:                                  | 1.44                                       | 1.53   | .23:                         | 24 $\pm$ 1       |
| PKS 0424-13 | 2.16     | 18.7 $\pm$ .2          | 30.88 $\pm$ .08  | 1.89                                   | 1.80 $\pm$ .01                             | 1.45   | .79                          | 21 $\pm$ 2       |
| 1108+285    | 2.19     | 21:                    | 29.97:   |  | 1.77                                       |  |                              | 19               |
| B1225+31.7  | 2.23     | 16.2 $\pm$ .3          | 31.90 $\pm$ .12  | 1.13                                   | 0.89 $\pm$ .08                             | 1.19   | .40                          | 57 $\pm$ 12      |
| 4C 25.05    | 2.34     | 18.7 $\pm$ .2          | 30.93 $\pm$ .08  | 1.84                                   | 1.56 $\pm$ .05                             | 1.26   | .53                          | 25 $\pm$ 2       |
| 5C 2.56     | 2.38     | 20.5:                  | 30.21:   | 1.96                                   | 1.63 $\pm$ .01                             |  | .33                          | 35 $\pm$ 1       |
| 2256+017    | 2.66     | 19.3 $\pm$ .4          | 30.76 $\pm$ .16  | 1.79                                   | 1.48 $\pm$ .11                             | 1.15   | .34                          | 17 $\pm$ 2       |
| PHL 957     | 2.69     | 16.8 $\pm$ .1          | 31.76 $\pm$ .04  | 1.54                                   | 1.11                                       | 1.26   | .28                          | 35               |
| 4C 05.34    | 2.86     | 18.3 $\pm$ .2          | 31.20 $\pm$ .08  | 1.79                                   | 1.47 $\pm$ .05                             | 1.13   | .33                          | 20 $\pm$ 3       |
| 0830+115    | 2.97     | 19.2 $\pm$ .2          | 30.86 $\pm$ .08  | 1.87:                                  | 1.75 $\pm$ .05                             |  | .38:                         | 24 $\pm$ 3       |
| 0938+119    | 3.19     | 20.2 $\pm$ .2          | 30.50 $\pm$ .08  |  | 1.76 $\pm$ .09                             |  | .50                          | 13 $\pm$ 2       |
| 0H 471      | 3.39     | 19.1 $\pm$ .2          | 30.97 $\pm$ .08  | 1.86                                   | 1.31 $\pm$ .10                             |  | .31                          | 15 $\pm$ 2       |
| 0Q 172      | 3.53     | 17.8 $\pm$ .1          | 31.51 $\pm$ .04  | 1.53                                   | 1.14 $\pm$ .05                             |  | .37                          | 40 $\pm$ 6       |

Error bars are given where they are known. Values suffixed by : indicate estimated uncertainty  $\pm 50\%$ .

emission lines. The continuum magnitudes were measured on Oke's  $AB_v$  system ( $AB_v = -2.5 \log F_v - 48.60$ ) at an observed wavelength corresponding to the rest wavelength  $\lambda_0 = 1450 \text{ \AA}$ . This wavelength was chosen as an emission-line-free region visible in all of the spectra taken in the initial sample. It was then assumed that the redshifts are cosmological, and a conversion of magnitudes to continuum luminosities (per unit frequency interval) for the case  $q_0 = +1$  was made, based on the relation  $\log L_{\text{cont}} = 38.19 - AB_v/2.5 + \log [z^2/(1+z)]$ . If  $q_0$  is in fact not equal to +1, redshift-dependent deviations in the computed luminosity will introduce scatter into any correlations present.

Figure 2 shows the correlation between the continuum luminosity and the equivalent width (in the rest frame) of C IV  $\lambda 1550$ . Similar correlations were found for the Ly $\alpha$  and C III]  $\lambda 1909$  equivalent widths, but more careful measurements were possible for the C IV line because it is generally stronger than C III] and does not suffer from the blending and absorption which often confuse the Ly $\alpha$  profile. Quasars having steep radio spectra, flat radio spectra, and concave or non-existent radio spectra are shown as different symbols in Figure 2. The flat-spectrum QSOs show the tightest

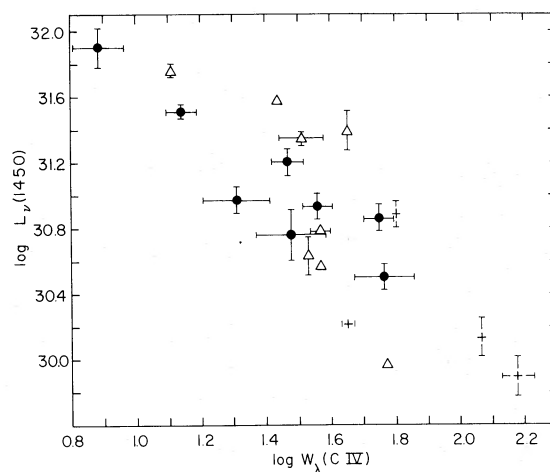


FIG. 2.—The relationship between the computed continuum luminosity at 1450  $\text{\AA}$  and the equivalent width of C IV  $\lambda 1550$  in the rest frame. The symbols have the same meaning as in Fig. 1.

correlation, while the steep-spectrum QSOs fit onto the lower luminosity end of this correlation. The radio-quiet and concave-spectrum QSOs show considerably more scatter, or at least a different slope. This is in general agreement with the results of Setti and Woltjer (1973a) and of Stannard (1973). A least-squares fit to the points on Figure 2 gives the relation  $\log L_{\text{cont}} = 33.34 - 1.57 \log W_{\lambda}$ . This means that the luminosity of the C IV line scales as about the one-third power of the continuum luminosity.

The four lowest-redshift QSOs in Table 1 were observed in an effort to extend the redshift range of the sample after the  $\log L_{\text{cont}} - \log W_{\lambda}$  (C IV) correlation began to emerge. These QSOs were picked from the DeVeny, Osborn, and Janes (1971) catalog without regard to the equivalent widths of their emission lines, and the observed correlation is not changed significantly

if they are left out of the sample. Nor is the correlation greatly changed if the luminosities are calculated for an empty universe with  $q_0 = 0$ ; the slope is decreased from  $-1.57$  to  $-1.73$ , but the correlation coefficient is only slightly increased from 0.82 to 0.84.

Three spectra illustrating the great range of these equivalent widths are illustrated in Figure 3. The data for B1225+31.7 are taken from Wampler *et al.* (1977). Other examples of these spectra have been previously published by Wampler *et al.* (1973a), Strittmatter *et al.* (1973), Coleman *et al.* (1976), and Baldwin *et al.* (1974).

The relationship between the continuum luminosity and the C IV  $\lambda 1550$  full width at half-maximum intensity (FWHM, in the rest frame) is shown in Figure 4. No correlation is evident for the sample as a whole, but the flat-spectrum sources do seem to be correlated in the sense that the more luminous QSOs

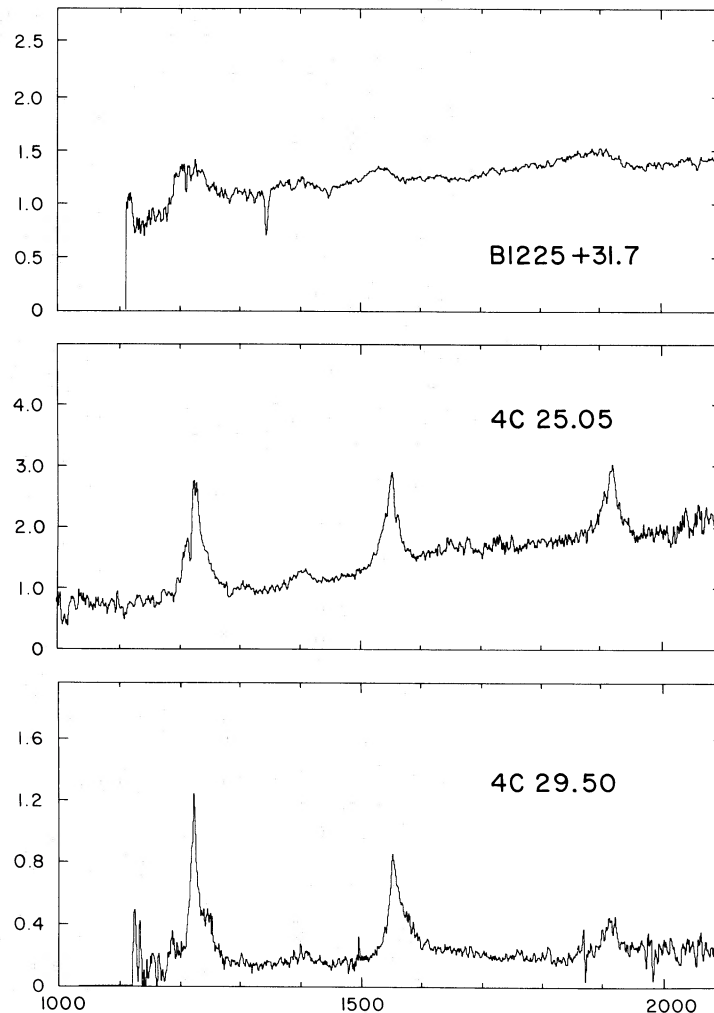


FIG. 3.—Representative spectra of three QSOs illustrating the great range in the equivalent widths of the emission lines. The abscissae are the rest wavelengths in angstroms and the ordinates are the observed fluxes in units of  $10^{-26}$ ,  $10^{-27}$ , and  $10^{-27}$  ergs  $\text{cm}^{-2} \text{s}^{-1} \text{H}_3^{-1}$  for B1225+31.7, 4C 25.05, and 4C 29.50, respectively.

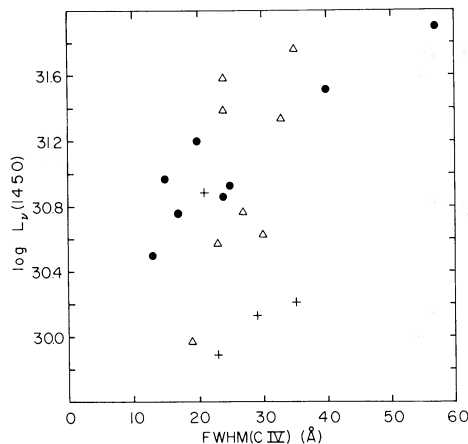


FIG. 4.—The relationship between the computed continuum luminosity at 1450 Å and the full width at half-maximum intensity (FWHM) of C IV  $\lambda$ 1550 in the rest frame. The symbols have the same meaning as in Fig. 1.

have broader emission lines. A similar plot of continuum luminosity against the  $L\alpha$ /C IV intensity ratio shows no correlations for any of the subsamples.

#### IV. DISCUSSION

In the most naive interpretation of the general model where QSO mass loss is driven by radiation pressure, one might expect that the more luminous QSOs would expel material more violently and thus produce broader emission lines, and Perry (1976) has found a weak correlation between absorption-line velocities (relative to the emission-line redshift) and the continuum luminosity. There are obviously many more parameters in the problem (the mass-to-luminosity ratio, for instance) that could easily destroy any simple relationship. Perhaps this is why only one type of QSO (those with flat radio spectra) shows any correlation whatsoever between luminosity and line widths. Even this result is based on only eight points and cannot be considered well established.

The  $L\alpha$  equivalent widths listed in Table 2 show the familiar result that not all of the ionizing photons are absorbed (compare  $W_\lambda \approx 30$ – $180$  Å in Table 2 to  $W_\lambda = 410 \tau$  [Lyman continuum edge] Å, the result of Davidson 1973). This implies that either the gas is optically thin in the Lyman continuum or, if it is optically thick, it cannot be arranged in a shell which completely covers the continuum source. The latter explanation would seem to be required in order to also account for the presence of the Mg II  $\lambda$ 2800 emission line in the spectra of lower-redshift QSOs (Baldwin *et al.* 1976; Oke 1974; Davidson 1973). The observed correlations between the equivalent widths and the continuum luminosity cannot be explained by a model in which the range of line strengths is related only to the differences in the continuum luminosities. For both the  $L\alpha$  and C IV lines we observe  $W_\lambda \propto L_{\text{cont}}^{-2/3}$ . If the gas is in all cases optically thin we expect  $W_\lambda(L\alpha) \propto L_{\text{cont}}^{-1}$ . If the gas is not extremely highly ionized, as is implied by the presence of the

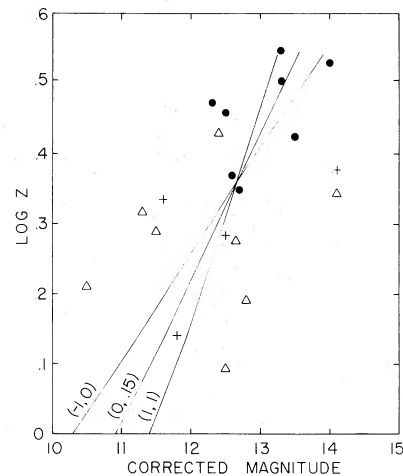


FIG. 5.—Redshift-magnitude diagram for the QSOs included in this study after they have been corrected to a standard continuum luminosity as described in the text. The symbols have the same meaning as in Fig. 1. The three lines are the predicted relationship for three combinations of  $(q_0, \sigma_0)$  taken from Refsdal, Stabell, and de Lange (1967).

C III]  $\lambda$ 1909 emission line, Davidson gives  $I(\text{C IV})/I(L\alpha) \propto L_{\text{cont}}$ ; so  $W_\lambda(\text{C IV})$  should stay about constant, contrary to the observations. If the gas is optically thick, we expect  $W_\lambda(L\alpha \text{ recombination}) \approx \text{constant}$ . For this case Davidson gives  $I(L\alpha \text{ collisional})/I(L\alpha \text{ recombination}) \propto L_{\text{cont}}^{-0.4}$ , so that the total  $L\alpha$  emission (which is about half recombination and half collisionally excited in Davidson's models) would be something like  $W_\lambda \propto L_{\text{cont}}^{-0.2}$ . In addition, in these models  $I(\text{C IV})/I(L\alpha) \propto L_{\text{cont}}^{0.9}$ , so that we expect  $W_\lambda(\text{C IV}) \propto L_{\text{cont}}^{-0.3}$  or even more nearly constant depending on the level of ionization. These dependences too are not very consistent with the observations. It is not surprising that this very simple model fails to fit the observations, and a more detailed analysis is under way in an attempt to estimate some of the physical parameters of these QSOs.

The strong correlation between the equivalent widths and the continuum luminosity was not expected, and the QSOs in the sample were chosen without any prior consideration of their emission-line strengths. It is still quite possible, though, that selection effects have led to the observed correlation. The computed luminosities depend on both the apparent magnitude and the distance indicated by the redshift, but for the redshift range used here most of the range in luminosities results from the range in the apparent magnitudes observed rather than from the range in the distances. Thus, the most luminous QSOs are also the ones with the brightest apparent magnitudes, and the least luminous QSOs are the apparently faintest ones. A plot of the apparent magnitudes against the equivalent widths shows nearly as strong a correlation as the one shown in Figure 2. It is quite conceivable that redshifts of faint QSOs would be found preferentially among those having strong emission lines; so points would not be expected to fall in the lower left

corner of Figure 2. But one would still expect to find bright QSOs with strong emission lines that would populate the upper right corner of Figure 2. The estimates of emission-line strengths given by Chan and Burbidge (1975) combined with the apparent magnitudes given by Sandage (1972) suggest that there are in fact some bright, strong-lined QSOs; but the one bright QSO that is called "strong-lined" and is included in the present sample is OQ 172, which is found here to have relatively weak emission lines. My results clearly need to be checked on the basis of quantitative measurements rather than rough estimates. A way to avoid selection effects in the future would be to make these measurements for all of the QSOs found in some complete radio sample.

Even if the correlation between the continuum luminosities and the equivalent width is not due to a selection effect, it still does not necessarily argue for cosmological redshifts. This is because there is also the correlation with the apparent magnitudes as described above, which indicates that even if these QSOs are all at the same distance (irrespective of their redshifts), there is still a tight relationship between the luminosities and the equivalent widths. A relationship with much less scatter or one extending over a much greater range in redshifts will be required in order to clearly separate out any redshift-dependent effects.

In spite of these problems, we can still use the  $\log L_{\text{cont}} - \log W_{\lambda}$  relationship to correct all of the observed objects to a standard luminosity and plot a new redshift-magnitude diagram. The result is shown

in Figure 5, where the abscissa  $m_{\text{corr}} = AB_{\nu} - 3.93 \log W_{\lambda}$  (C IV). This is equivalent to a plot of the redshifts against the residuals from the best fit to the  $\log L_{\text{cont}} - \log W_{\lambda}$  correlation. If the wrong value of  $q_0$  has been used in working out  $L_{\text{cont}}$ , then there should be a redshift-dependent deviation from the predicted relationship for  $q_0 = +1$  which would indicate the correct value of  $q_0$ . Predicted relationships for the  $q_0 = +1$ ,  $\sigma_0 = 1$  case and for two other plausible cosmologies are shown in Figure 5. Although the scatter in the data is considerably reduced from that in Figure 1, the results are still noisy enough to be consistent with any of the values of  $q_0$  currently thought to be reasonable. It is the large scatter in the points corresponding to lower redshifts that particularly restricts the usefulness of this approach. Additional careful observations of several QSOs with lower redshifts, but where the C IV line can still be measured ( $z \approx 1.2-1.3$ ), and with flat radio spectra might tie down the low-redshift part of the range and allow further progress to be made.

I wish to thank Drs. E. J. Wampler, J. Perry, and R. Carswell for helpful discussions. I also thank several of my colleagues, particularly Joe Wampler, for allowing me to use the Lick Observatory data banks. This research was partially supported by NSF grant GP-29684. I am grateful to the staff of the Max Planck Institute for Physics and Astrophysics in München for their hospitality while this paper was being written.

## REFERENCES

- Argue, N., Ekers, R. D., Farnaroff, B. L., Hazard, C., Ryle, M., Shakeshaft, J. R., Stockton, A., and Webster, A. S. 1974, *M.N.R.A.S.*, **168**, 1P.
- Bahcall, J., and Hills, R. 1973, *Ap. J.*, **179**, 699.
- Baldwin, J. A., Burbidge, E. M., Burbidge, G. R., Hazard, C., Robinson, L. B., and Wampler, E. J. 1974, *Ap. J.*, **193**, 513.
- Baldwin, J. A., Burbidge, E. M., Hazard, C., Murdoch, H. S., Robinson, L. B., and Wampler, E. J. 1973, *Ap. J.*, **185**, 739.
- Baldwin, J. A., Smith, H. E., Burbidge, E. M., Hazard, C., Murdoch, H. S., and Jauncey, D. L. 1976, *Ap. J. (Letters)*, **206**, L83.
- Beaver, E. A., Harms, R., Hazard, C., Murdoch, H. S., Carswell, R. F., and Strittmatter, P. A. 1976, *Ap. J. (Letters)*, **203**, L5.
- Burbidge, G. R. 1973, *Nature Phys. Sci.*, **246**, 17.
- Carswell, R. F., and Strittmatter, P. A. 1973, *Nature*, **242**, 394.
- Chan, Y.-W. T., and Burbidge, E. M. 1975, *Ap. J.*, **198**, 45.
- Coleman, G., Carswell, R. F., Strittmatter, P. A., Williams, R. E., Baldwin, J., Robinson, L. B., and Wampler, E. J. 1976, *Ap. J.*, **207**, 1.
- Davidson, K. 1973, *Ap. J.*, **181**, 1; **186**, 399.
- DeVeny, J. B., Osborn, W. H., and Janes, K. 1971, *Pub. A.S.P.*, **83**, 611.
- Fanti, C., Fanti, R., Ficarra, A., Formigini, L., Giovannini, G., Lari, C., and Padrielli, L. 1975, *Astr. Ap. Suppl.*, **19**, 143.
- Gearhart, R., et al. 1974, *Nature*, **249**, 743.
- Hoskins, D. G., Murdoch, H. S., Adgie, R. L., Crowther, J. H., and Gent, H. 1974, *M.N.R.A.S.*, **166**, 235.
- Murdoch, H. S. 1974, *Nature*, **247**, 443.
- Oke, J. B. 1974, *Ap. J. (Letters)*, **189**, L47.
- Perry, J. J. 1976, preprint.
- Refsdal, S., Stabell, R., and de Lange, F. G. 1967, *Mem. R.A.S.*, **71**, 143.
- Robinson, L. B., and Wampler, E. J. 1971, *Pub. A.S.P.*, **84**, 161.
- Sandage, A. 1972, *Ap. J.*, **178**, 25.
- Setti, G., and Woltjer, L. 1973a, *Ap. J. (Letters)*, **181**, L61.
- . 1973b, *Proceedings of Sixth Texas Symposium on Relativistic Astrophysics (Ann. NY Acad. Sci.*, **224**, 1).
- Stannard, D. 1973, *Nature*, **236**, 295.
- Stone, R. P. S. 1974, *Ap. J.*, **193**, 135.
- Strittmatter, P. M., Carswell, R. F., Burbidge, E. M., Hazard, C., Baldwin, J. A., Robinson, L., and Wampler, E. J. 1973, *Ap. J.*, **183**, 767.
- Wampler, E. J., Baldwin, J. A., Burke, W. L., Robinson, L. B., and Hazard, C. 1973a, *Nature*, **246**, 203.
- Wampler, E. J., Robinson, L. B., Baldwin, J. A., and Burbidge, E. M. 1973b, *Nature*, **243**, 336.
- Wampler, E. J., Robinson, L. B., Baldwin, J. A., Burbidge, E. M., Strittmatter, P. A., Carswell, R. F., Williams, R., and Coleman, G. 1977, in preparation.

JACK A. BALDWIN: Institute of Astronomy, Madingley Road, Cambridge CB3 0HA, England